Supporting Information

Tikhonova et al. 10.1073/pnas.0906601106

SI Materials and Methods

Overproduction and Purification of Proteins. For large-scale purification, soluble AcrA and MacA were subcloned and expressed from pET21d(+) vector (Novagen). EmrA that does not have the N-terminal transmembrane segment but contains the C-terminal 6His-tag was constructed as described in ref. 1.

All three 6His-tagged soluble MFPs (MacA, AcrA, and EmrA) and AcrA mutants were expressed and purified from cytoplasmic fraction of *E. coli* BL21(DE3) cells harboring respective plasmids. The expression was induced by 1 mM IPTG, and proteins were purified by using metal affinity chromatography, as described in ref. 2. After purification, proteins were dialyzed in buffer containing 50% glycerol, 20 mM Hepes-KOH (pH 7.7), 500 mM NaCl, and 1 mM PMSF and were kept at −20 °C until needed.

Purified proteins were separated by electrophoresis on SDS-polyacrylamide gels and visualized by Coomassie Brilliant Blue (CBB) or silver nitrate staining. The protein concentration was determined by using a Protein DC Assay (Bio-Rad) and by ImageQuant (GE Healthcare) analysis of the CBB-stained gels with BSA as a standard (3).

Amino and Thiol Coupling of MFPs to Biosensor Chips. For both amino- and thiol-coupling procedures, the CM5 chip surfaces were activated with 0.05 M *N*-hydroxysuccinimide and 0.2 M *N*-ethyl-*N*′-(3-diethylaminopropyl)carbodiimide (BIAcore). For amino coupling, ligands were injected over surfaces immediately after activation. For thiol coupling, the activated CM5 chip was further treated with 2-(2-pyridinyldithio)ethaneamine hydrochloride as recommended by the manufacturer (BIAcore). Disulfide bonds of AcrAS362C dimers were reduced by using Tris[2-carboxyethyl]phosphine hydrochloride disulfide reducing gel (Pierce). After immobilization by amino coupling, the excess of reactive groups was blocked by injecting 0.5 M ethanolamine HCl (pH 8.0). The excess of disulfides on surfaces was blocked by injecting 10 mM cysteine in 100 mM sodium acetate buffer (pH 4.8) containing 1 M NaCl. Both amino- and thiol-coupling immobilizations were conducted in the running buffer containing 20 mM Mes-KOH (pH 5.8), 150 NaCl, and 0.05% DDM (Mes-DDM), with MFPs at concentrations of 0.003 mg/mL in 10 mM sodium acetate (pH 4.8). The CM5 chip contains four chambers, three of which contained the immobilized MFPs (ligands), whereas the fourth, control surface was activated and processed in the same way, but protein was omitted during the immobilization step.

The surface density of MFPs was manipulated by changing the activation time and the concentration of a ligand as recommended by the manufacturer. Although immobilization of MFPs was carried out at very low protein concentrations, the efficient cross-linking required acidic pH 4.8. The acidic pH was shown previously to promote oligomerization of AcrA (4, 5). Thus, it is likely that MFPs were immobilized onto the surface as a mixture of monomers and oligomers. After immobilization, proteins were stable for at least 2 weeks without significant loss of binding capacity.

Analysis of AcrA and MacA structures (5, 6) showed that ≈75% of lysine residues in these proteins are located outside the α-hairpin, the domain implicated in interactions with TolC (7). Furthermore, lysine residues of the α-hairpin, lipoyl domain, and α-β-barrel domain of both AcrA and MacA are not accessible to trypsin (3, 5). Sequence alignment and structure modeling of EmrA indicate that EmrA follows the same trend. Thus, during amino-coupling procedure, MFPs are likely to be cross-linked to the surface via their N and C termini, with their TolC-binding α-hairpins extended away from the surface. In agreement with this analysis, AcrA mutant lacking the α-hairpin did not bind TolC (Fig. S3).

Kinetic Modeling of TolC–MFP and MFP–MFP Interactions. We considered only the simplest models that would be compatible with at least two distinct events during both protein binding and dissociation. These five models are: (*i*) HL, in which different protein populations on chip surface have different kinetic properties; (*ii*) ligand-induced conformational change, wherein conformational change occurs on the same time scale as ligand binding; (*iii*) heterogeneous analyte, wherein different protein populations in solution have different kinetic properties; (*iv*) bivalent analyte, where multiple analytes bind independently at nonidentical sites; and (*v*) ST, which postulates sequential binding of two soluble molecules to one immobilized on the surface. Distinguishing between these models is possible if the data are fit globally; that is, by fitting all sensorgrams, obtained at various protein concentrations, by using the same set of parameters (8).

Schematic representation and equations relevant to the HL model, which is the model on which the discussion of MFP–TolC interactions is based, are given here:

$$MFP_1 + TolC \underset{k_{-1}}{\overset{k_1}{\rightleftharpoons}} MFP_1{\cdot}TolC;$$

$$\frac{\partial(MFP_1{\cdot}TolC)}{\partial t} = k_1[MFP_1][TolC] - k_{-1}[MFP_1{\cdot}TolC]$$

$$MFP_2 + TolC \underset{k_{-2}}{\overset{k_2}{\rightleftharpoons}} MFP_2{\cdot}TolC;$$

$$\frac{\partial(MFP_2{\cdot}TolC)}{\partial t} = k_2[MFP_2][TolC] - k_{-2}[MFP_2{\cdot}TolC]$$

total response,

$$R_t = [MFP_1{\cdot}TolC] + [MFP_2{\cdot}TolC],$$

where MFP_1 and MFP_2 are concentrations of the two populations of the immobilized MFP; $[TolC]$ is the concentration of TolC; $[MFP_1{\cdot}TolC]$ and $[MFP_2{\cdot}TolC]$ are the different complexes; k_{-1}, k_{-2}, k_1, and k_2 are microscopic rate constants; and R_t is the total SPR response, which is directly proportional to $[MFP_1{\cdot}TolC] + [MFP_2{\cdot}TolC]$.

The kinetic scheme and relevant equations for the ST model used to fit EmrA oligomerization sensorgrams are given here:

$$EmrA_i + EmrA_s \underset{k_{-1}}{\overset{k_1}{\rightleftharpoons}} EmrA_i{\cdot}EmrA_s; \quad \frac{\partial(EmrA_i{\cdot}EmrA_s)}{\partial t} = k_1[EmrA_i][EmrA_s] - k_{-1}[EmrA_i{\cdot}EmrA_s]$$

$$EmrA_i{\cdot}EmrA_s + EmrA_s \underset{k_{-2}}{\overset{k_2}{\rightleftharpoons}} EmrA_i{\cdot}2EmrA_s; \quad \frac{\partial(EmrA_i{\cdot}2EmrA_s)}{\partial t} = k_2[EmrA_s][EmrA_i{\cdot}EmrA_s] - k_{-2}[EmrA_i{\cdot}2EmrA_s],$$

$$B_{max} = [EmrA_i] + [EmrA_i{\cdot}EmrA_s] + [EmrA_i{\cdot}2EmrA_s]$$

where $EmrA_i$ and $EmrA_s$ are the immobilized and soluble EmrA, respectively; k_{-1}, k_{-2}, k_1, and k_2 are microscopic rate constants, and B_{max} is the total number of the available binding sites on the surface.

1. Borges-Walmsley MI, et al. (2003) Identification of oligomerization and drug-binding domains of the membrane fusion protein EmrA. *J Biol Chem* 278:12903–12912.
2. Zgurskaya HI, Nikaido H (1999) AcrA is a highly asymmetric protein capable of spanning the periplasm. *J Mol Biol* 285:409–420.
3. Tikhonova EB, Devroy VK, Lau SY, Zgurskaya HI (2007) Reconstitution of the Escherichia coli macrolide transporter: The periplasmic membrane fusion protein MacA stimulates the ATPase activity of MacB. *Mol Microbiol* 63:895–910.
4. Ip H, Stratton K, Zgurskaya H, Liu J (2003) pH-induced conformational changes of AcrA, the membrane fusion protein of Escherichia coli multidrug efflux system. *J Biol Chem* 278:50474–50482.
5. Mikolosko J, Bobyk K, Zgurskaya HI, Ghosh P (2006) Conformational flexibility in the multidrug efflux system protein AcrA. *Structure* 14:577–587.
6. Yum S, et al. (2009) Crystal structure of the periplasmic component of a tripartite macrolide-specific efflux pump. *J Mol Biol* 387:1286–1297.
7. Lobedanz S, et al. (2007) A periplasmic coiled-coil interface underlying TolC recruitment and the assembly of bacterial drug efflux pumps. *Proc Natl Acad Sci USA* 104:4612–4617.
8. Schasfoort RBM, Tudos AJ, eds (2008) *Handbook of Surface Plasmon Resonance* (RSC Publishing, Cambridge, UK).

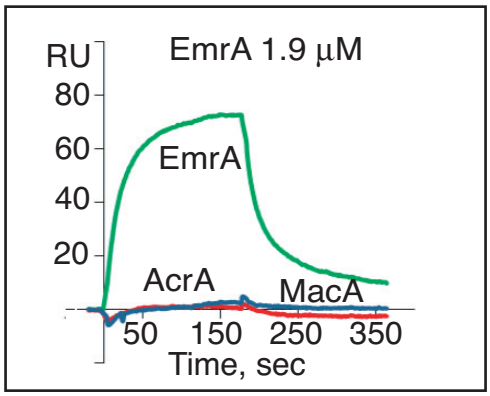

Fig. S1. Oligomerization of MFPs is highly specific. EmrA (1.9 μM) in Mes-DDM running buffer (pH 5.8) was injected over the surfaces with immobilized EmrA (154 response units; green), AcrA (121 response units; blue), and MacA (200 response units). No heterooligomerization was detected between these homologous MFPs.

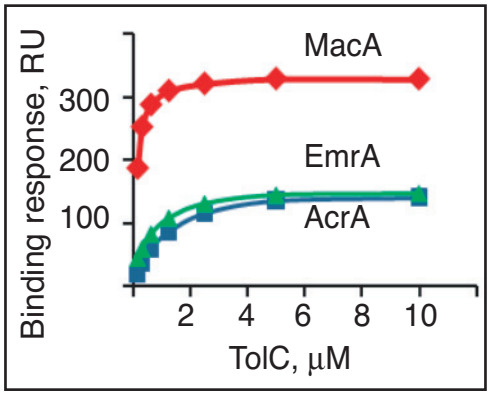

Fig. S2. Saturation of immobilized MFPs with TolC. MFPs were immobilized to densities of 75 response units of AcrA (blue), 108 response units of EmrA (green), and 352 response units of MacA (red). TolC was injected in the Mes-DDM running buffer (pH 5.8) at concentrations increasing from 0.16 to 10.0 μM (50 μL/min for 1 min). MacA surface was saturated at 1.25 μM TolC, whereas EmrA and AcrA surfaces were saturated at 5.0 μM TolC.

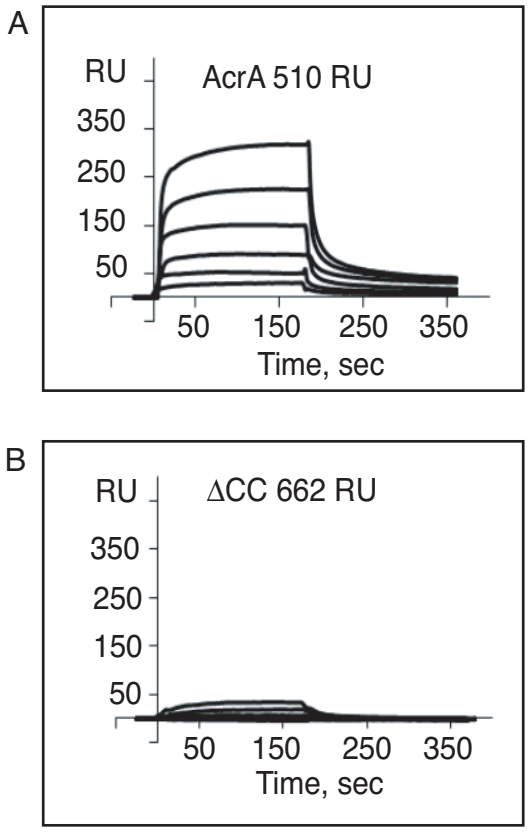

Fig. S3. Interactions between immobilized AcrA and TolC are mediated by the α-helical hairpin domain. AcrA and its mutant lacking the α-helical hairpin (ΔCC) were immobilized onto a CM5 surface to densities of 510 response units of AcrA (*A*) and 662 response untis of AcrAΔCC (*B*). TolC was injected in the Mes-DDM running buffer (pH 5.8) at concentrations increasing from 0.06 to 2.0 μM. No significant TolC binding was detected on the surface containing AcrAΔCC.

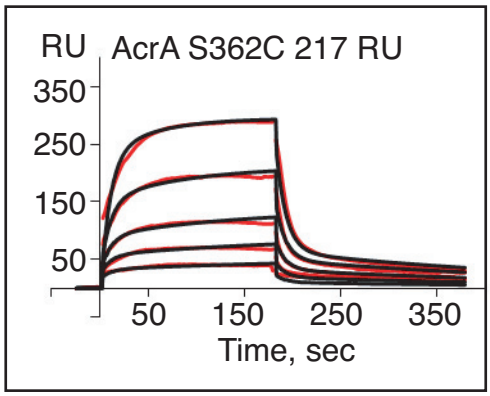

Fig. S4. Heterogeneity of AcrA is intrinsic to the protein. AcrAS362C mutant was immobilized on the CM5 chip to the density of 217 response units by using thiol-disulfide exchange. Data were normalized to the protein-free control surface, which was subject to the mock cross-linking procedure. TolC was injected in the Mes-DDM running buffer (pH 5.9) at concentrations increasing from 0.125 to 2.0 μM. The best fit for AcrAS362C was obtained by using the HL model (black lines) with $K_{d1} = 0.36$ μM and $K_{d2} = 22.2$ μM for the fast and slow complexes, respectively (Table S1). The lower affinity of TolC binding to AcrAS362C could be due to the differences in coupling chemistry and mutation in AcrA.

Table S1. Kinetic parameters of TolC–MFP interactions

Ligand	Density, response units	TolC, μM	k_1, $M^{-1}\,s^{-1}$	k_{-1}, s^{-1}	K_{d1}, μM (slow)	k_2, $M^{-1}\,s^{-1}$	k_{-2}, s^{-1}	K_{d2}, μM (fast)	% slow*	% fast*	Residuals, χ^2
EmrA	108	0.06–2.00	$(6.1 \pm 0.08) \times 10^4$	$(4.9 \pm 0.7) \times 10^{-3}$	0.08	$(11.0 \pm 0.6) \times 10^4$	0.14 ± 0.02	1.27	29 ± 5	71 ± 3	1.7
EmrA	1,553	0.04–1.28	$(5.21 \pm 0.09) \times 10^4$	$(5.2 \pm 0.7) \times 10^{-3}$	0.10	$(20.3 \pm 0.3) \times 10^4$	0.047 ± 0.009	0.33	13 ± 1	87 ± 2	77.4
AcrA	75	0.06–2.00	$(2.84 \pm 0.04) \times 10^4$	$(3.1 \pm 0.4) \times 10^{-3}$	0.11	$(5.93 \pm 0.5) \times 10^4$	0.123 ± 0.03	2.08	28 ± 4	72 ± 2	0.9
AcrA	2,225	0.04–1.28	$(3.75 \pm 0.04) \times 10^4$	$(3.7 \pm 0.3) \times 10^{-3}$	0.10	$(6.17 \pm 0.1) \times 10^4$	0.083 ± 0.06	1.35	12 ± 1	88 ± 10	125
MacA	2,663	0.04–1.28	$(4.85 \pm 0.05) \times 10^4$	$(2.1 \pm 0.3) \times 10^{-3}$	0.04	$(22.9 \pm 1.6) \times 10^4$	0.047 ± 0.009	0.2	58 ± 4	42 ± 3	317
AcrA S362C	217	0.12–2.0	$(0.84 \pm 0.03) \times 10^4$	$(3.0 \pm 0.4) \times 10^{-3}$	0.36	$(0.45 \pm 0.1) \times 10^4$	0.097 ± 0.07	22.2	4 ± 0.4	96 ± 19	34.6

All data were fit globally by using the HL model, where k_{-1}, k_{-2}, k_1, and k_2 are microscopic rate constants, and R_t is the total SPR response. Equilibrium dissociation constants (K_d) were calculated from the ratio of the dissociation and association rate constants.
*Fractions of R_t corresponding to the slow and fast complexes.